J Mater Sci (2013) 48:4274–4283
DOI 10.1007/s10853-013-7241-9

Synthesis, characterization, and catalytic activity of nitridated magnesium silicate catalysts

Katabathini Narasimharao · Mohamed Mokhtar · Sulaiman N. Basahel · Shaeel A. Al-Thabaiti

Received: 10 December 2012 / Accepted: 13 February 2013 / Published online: 22 February 2013

Abstract Amorphous and crystalline magnesium silicates (MgSils) were prepared by sol–gel and template-assisted hydrothermal synthesis methods, respectively. The obtained materials were nitridated with NH_3 at 300, 500, and 800 °C for 24 and 48 h generating nitridated MgSil catalysts. The catalysts were characterized by XRD, FTIR, TG–MS, N_2-physisorption, Hammett indicators, and elemental analysis methods. MgSils nitridated at 300 °C were found to be more active for the Knoevenagel condensation reaction, compared to those nitradated at 500 or 800 °C. A larger amount of nitrogen was incorporated in the framework of amorphous MgSil compared to the crystalline MgSil. FTIR analysis indicated the presence of NH_x species, which were known to form upon reaction between NH_3 and M-OH groups. It was also found that the presence of Si–OH and Mg–OH groups along with the basic $–NH_2$ functional groups is responsible for the enhanced catalytic activity of the low-temperature nitridated catalysts.

Introduction

A considerable amount of research has been focused on new types of silicates with tunable properties due to their potential application in many areas including catalysis, gas adsorption, and separation [1]. Natural or synthetic aluminum and/or magnesium silicates belonging to the clay minerals group have industrial importance due to their particular crystal structure, microfibrous morphology [2]. The magnesium ions in the crystal lattice of magnesium silicate clay-type materials are exchangeable with transition metal ions and the resultant materials are capable of adsorbing both acidic and basic ions [3]. These materials were tested as refining and purifying agents in the production of polyether polyols and found that they are excellent, deodorizing, potassium ion adsorbing agents [4]. Magnesium silicates, and its derivatives, were also used for advanced applications such as specific catalyst [5], fire-retardant painting material [6], and a template for the synthesis of carbon nanofibers [7].

The structure of naturally occurring MgSil (Sepiolite) is derived from talc-like ribbons that expand with a width of three pyroxene chains. Each ribbon is connected to the next through an inverted Si–O–Si bond, resulting in a staggered talc layer with a continuous tetrahedral sheet and a discontinuous octahedral sheet. The discontinuous nature of the octahedral sheet allows for the formation of rectangular, tunnel-like micropores, which run parallel to the fiber axis and are filled completely by zeolitic water under ambient conditions [8]. These characteristics of MgSil have some resemblance to those of zeolites, although zeolites are aluminosilicates. A US patent disclosed information about the synthesis and characterization of MgSil-resembling zeolites with a crystalline structure [9]. The framework of these materials is typically a pentasil structure similar to that of ZSM-5.

Corma and Martin-Aranda [10] reported that strong base catalysts can be prepared by substituting a part of the Mg ions located at the borders of the channels of MgSil with alkaline ions and those materials showed higher basicity than the alkaline X-zeolites. The authors also reported that these catalysts were able to catalyze the condensation of benzaldehydes with active methylene compounds at

K. Narasimharao (✉) · M. Mokhtar · S. N. Basahel · S. A. Al-Thabaiti
Department of Chemistry, Faculty of Science, King Abdulaziz University, P.O. Box 80203, Jeddah 21589, Kingdom of Saudi Arabia
e-mail: katabathini@yahoo.com

moderate temperatures. Conventional alkali metal-impregnated solid base catalysts have disadvantages such as alkali metal leaching, pore blocking of the molecular sieve host by the basic guests, and reusability [11]. Porous nitrides or oxynitrides have been recognized as a new family of basic catalysts [12]. These materials can be prepared by treating precursors like SiO_2, $SiCl_4$, or amorphous aluminophosphates with ammonia [13, 14]. The resulting materials (Si_2N_2O) and the so-called AlPONs have been found to be active in the Knoevenagel condensation of benzaldehyde with malononitrile. The basicity of these catalysts has been attributed to the presence of nitrogen atoms that are substituted for some of the oxygen atoms during ammonia treatment. Several research publications have been reported on preparation and application of strong basic zeolite catalysts [15–18]. El Haskouri et al. [19] described that it is possible to prepare ordered mesoporous silicon oxynitrides of the MCM-41 type. These materials showed high activity in the Knoevenagel condensation of benzaldehyde with active methylene compounds. Wu et al. [20] observed the improvement in surface basic property of BaO-MCM-41 and BaO-SBA-15 catalysts without losing any structural damage after bridging –NH functional groups by the nitridation process. Chino and Okubo [21] prepared mesoporous silicon oxynitride materials by nitridation. The results of their study indicated that the nitridation routes are dependent on the temperature of the thermal treatment as well as the presence of surface defect species on the surface.

Hammond et al. [22] compared the quantum calculations on amine-substituted HY zeolite clusters with the solid state ^{29}Si NMR spectra of corresponding materials to obtain the evidence for successful incorporation of nitrogen in the framework of HY zeolite. Recently, Wang et al. [23] prepared nitrogen-containing MgO-MCM-41 solid base material by nitridation of MgO-loaded mesoporous MCM-41. Nitridated catalyst shows improved activity when compared with its parent MgO-MCM-41 in the Knoevenagel condensation reaction and the Claisen–Schmidt reaction. In general, regardless of the nature of the porous materials, there is always a risk of structural damage after prolonged ammonia treatment at higher temperatures. Narasimharao et al. [24] reported the advantage of low temperature nitridation of zeolite beta to synthesize the novel family of base catalysts for the Knoevenagel condensation reaction. Small polar molecules, including ammonia, methanol, ethanol, or acetone, can access the tunnels of MgSil compounds, either by displacing the zeolitic water molecules or by filling the free space in the crystal lattice [8].

Here, we report the preparation of amorphous and crystalline magnesium silicon nitride catalysts by low-temperature nitridation with NH_3. The physico-chemical properties of the materials have been characterized by powder X-ray diffraction (XRD), N_2 physisorption, FTIR spectroscopy, TG–MS, Hammett indicator method, and elemental analysis techniques. The catalytic properties of the synthesized materials were explored in the Knoevenagel condensation of benzaldehyde with the malononitrile reaction. To the best of our knowledge, the preparation, characterization, and application of magnesium silicon nitride catalysts for the aforementioned reaction has not previously been reported.

Experimental section

Materials

All reagents were analytical grade and used as received without purification. Tetraethyl orthosilicate [$Si(OC_2H_5)_4$], magnesium nitrate [$Mg(NO_3)_2{\cdot}6H_2O$], magnesium chloride [$MgCl_2{\cdot}6H_2O$], tetra butyl ammonium bromide [$(C_3H_7)_4NBr$], hydrochloric acid, and sodium hydroxide solution were purchased from Aldrich, U.K.

Sol–gel preparation method

In sol–gel method (SiO_2:MgO mass ratio = 6:2), 32.4 mL of $Si(OC_2H_5)_4$ [TEOS] was mixed with 50 mL of ethanol. Then, 3 mL of 1 M HNO_3 was added drop wise to maintain pH 5.0. The solution was refluxed by agitating with a magnetic stirrer in an oil bath at 75 °C for 1 h to obtain a silica sol solution. A calculated amount of aqueous $Mg(NO_3)_2{\cdot}6H_2O$ was added to the refluxing solution, followed by 50 mL of distilled water. The refluxing of the final solution continued until a gel is formed (12 h). Then, the gel was transferred into a beaker and dried at 120 °C for 5 h followed by calcination at 500 °C in air for 5 h.

Hydrothermal preparation method

In the hydrothermal method (SiO_2:MgO mass ratio = 6:2), three solutions were prepared in three separate beakers; (a) 50 g of commercially available Ludox SM colloidal silica (30 wt% SiO_2, 0.56 wt% Na_2O) was mixed with 4.0 g of NaOH solution (50 wt% NaOH) and 50 g of H_2O; (b) 13 g of tetrabutyl ammonium bromide [$(C_3H_7)_4NBr$] was dissolved in 55 g of H_2O; (c) 5.1 g of $MgCl_2{\cdot}6H_2O$ dissolved in 50 g of H_2O. The solutions (a) and (b) were mixed thoroughly for 30 min, then solution (c) was added and the solution was mixed for another 30 min, so as to produce a transparent homogeneous mixture. The pH of the mixture was adjusted to 11 by adding 1 M NaOH solution. The mixture was then transferred into a stainless steel autoclave and stirred at 160 °C for 2 days under

autogenous pressure. The product was recovered by filtration and rinsed with copious amounts of distilled water, dried for 12 h in air, and then calcined at 500 °C for 5 h. We prepared magnesium silicates with SiO_2:MgO mass ratio of 6:2, because at this ratio these materials possessed better textural properties [9].

Nitridation of the magnesium silicate materials

The nitridation was performed with ammonia gas (flow rate = 60 mL min^{-1}) at temperatures between 300 and 800 °C for 24 and 48 h. Subsequently, the samples were cooled down to room temperature under nitrogen gas flow (60 mL min^{-1}). The following nomenclature is used for the sample codes:

MgSil is abbreviated for "magnesium silicate,"
SG denotes sol–gel,
HT denotes hydrothermal, and
N denotes a nitridated sample.

Three numbers following one of the former abbreviations represent the nitridation temperature in °C and the last two numbers represent the treatment time in hours.

Characterization

Powder X-ray diffraction patterns were collected on a Siemens-axs D5005 diffractometer using Cu Kα radiation. Nitrogen adsorption–desorption isotherms were recorded at liquid nitrogen temperature using a Quantachrome Autosorb-1 sorption analyzer. The FTIR spectra were collected on a Nicolet Nexus spectrometer equipped with a high temperature in situ chamber. TG–MS experiments (heating rate = 5 °C min^{-1} under flow of nitrogen gas) were performed using a SETARAM setsys-16/MS instrument. Elemental analysis of the nitridated samples for nitrogen was carried out using a Perkin-Elmer 2400 CHN elemental analyzer. Base strength was determined by Hammett indicators; approximately 25 mg of sample were shaken with 1 mL of a solution of Hammett indicator diluted in toluene and left to equilibrate for 2 h at which point no further color change was observed. The color on the catalyst was then noted. The following Hammett indicators were used: neutral red ($pK_{BH+} = 6.8$), phenolphthalein ($pK_{BH+} = 8.2$), Nile blue ($pK_{BH+} = 10.1$), Tropaeolin-O ($pK_{BH+} = 11$), 2,4-dinitroaniline ($pK_{BH+} = 15$), 4-chloro-2-nitroaniline ($pK_{BH+} = 17.2$), and nitroaniline ($pK_{BH+} = 18.4$). Hammett indicator measurements are usually performed using non-polar solvents; it was therefore deemed appropriate to use toluene in this instance, as a measure of the base strength of the catalyst under reaction conditions was to be determined. The base strength was presented as being stronger than the weakest indicator which exhibits a color change, but weaker than the strongest indicator that produces no change.

Knoevenagel condensation reaction

The Knoevenagel condensation test reactions were performed in a round-bottom flask, equipped with a magnetic stirrer and a reflux condenser. The flask containing a mixture of distilled benzaldehyde (4 mmol), malononitrile (4 mmol), and 10 mL of toluene was immersed in an oil bath to adjust the reaction temperature. Once the mixture reached the desired temperature (80 °C), 200 mg of dried catalyst (150 °C) was added into the flask. Samples of the reaction mixture were then periodically withdrawn by a filtering syringe and analyzed by an Agilent gas chromatograph equipped with a flame ionization detector (FID) detector and a HP-5 capillary column.

Results and discussion

The powder XRD patterns of as-synthesized MgSilSG, MgSilHT, and samples calcined at 500 °C are shown in Fig. 1. The as-synthesized and calcined samples of MgSilSG are amorphous in nature; in contrast, the MgSilHT samples are highly crystalline. After calcination at 500 °C, MgSilHT showed major reflections at $2\theta = 7.9°$, 8.8°, 23.0°, 23.2°, 23.7°, and 23.9°. These peaks correspond to the results published by the International Zeolite Association [25] for the diffraction pattern of ZSM-5 with the MFI structure. No diffraction peaks indicating the presence of MgO or $Mg(OH)_2$ were observed for either of the samples, which implies that the magnesium ions were intercalated in the silicate network during the preparation. The XRD patterns of MgSilSG and MgSilHT samples nitridated for 24 h at 300, 500, and 800 °C are shown in Fig. 2a and b, respectively. No significant changes were observed in either the MgSilSG or MgSilHT samples after nitridation and each maintained their amorphous and crystalline nature even after nitridation at 800 °C. These results indicate that no structural damage occurred as a result of the high-temperature treatment and the ordered MFI structure of MgSilHT is preserved after the high-temperature nitridation.

The nitrogen physisorption isotherms of MgSilSG, MgSilSGN30024, MgSilHT, and MgSilHTN30024 are presented in Fig. 3. The isotherms of the MgSilSG, MgSilSGN30024, and MgSHT samples were of type IV, with a hysteresis in the 0.85–1.0 P/P^0 region, typical of mesoporous materials. The isotherm of the MgSHTN30024 sample showed a different pattern of the desorption path in the 0.75–1.0 P/P^0 region. The appearance of a well-defined hysteresis loop associated with irreversible capillary

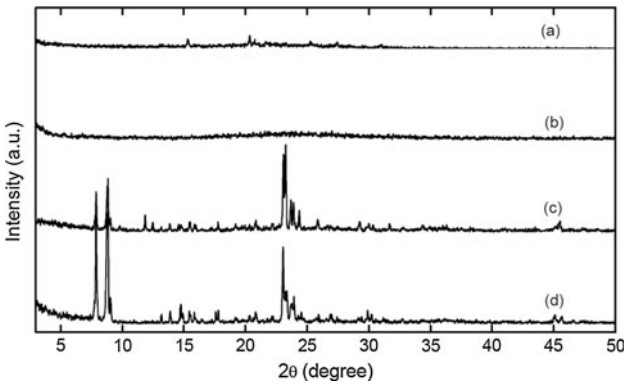

Fig. 1 Powder XRD patterns of (*a*) as-synthesized MgSilSG, (*b*) MgSilSG calcined at 500 °C, (*c*) as-synthesized MgSilHT, and (*d*) MgSilHT calcined at 500 °C

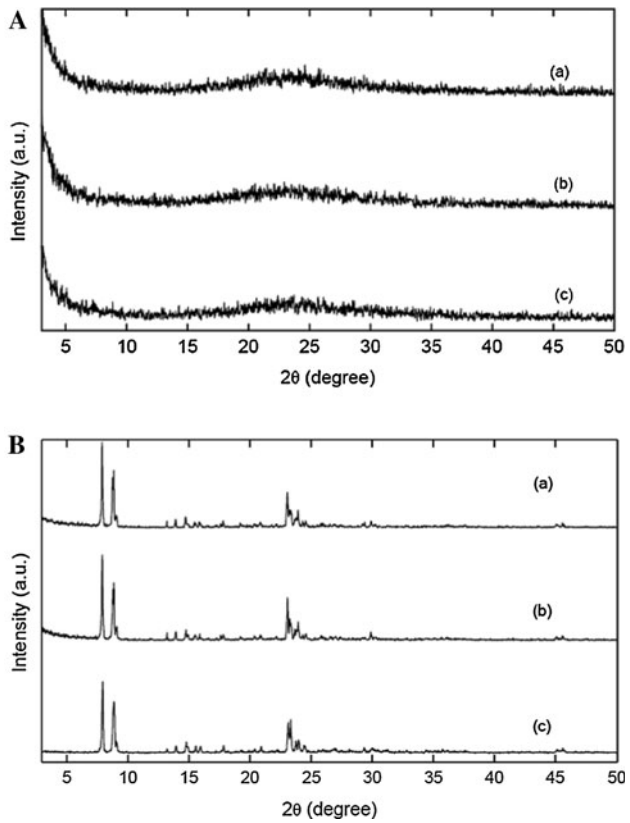

Fig. 2 **A** Powder XRD patterns of MgSilSG treated with ammonia for 24 h at temperatures (*a*) 300 °C, (*b*) 500 °C, (*c*) 800 °C; **B** powder XRD patterns of MgSilHT treated with ammonia for 24 h at temperatures (*a*) 300 °C, (*b*) 500 °C, and (*c*) 800 °C

condensation in the mesopores of the P/P^0 region from 0.85 to 1.0 suggests the presence of mesoporosity arising from non-crystalline voids and spaces formed by interparticle contacts in the sample. The specific surface areas, specific pore volumes, and nitrogen content of the calcined MgSilSG, MgSilHT, and of the nitridated samples are listed in Table 1. The specific surface area of MgSilSG

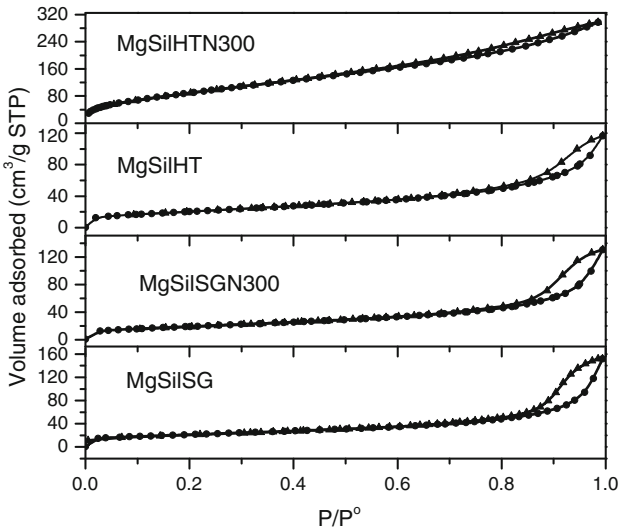

Fig. 3 N_2 physisorption isotherms of selected magnesium silicate samples

sample calcined at 500 °C was determined to be 320 $m^2\ g^{-1}$, which is higher than the metal supported sepiolite (a natural magnesium silicate) catalysts reported by Kitayama et al. [26]. The large specific surface area of MgSilSG may arise as a result of its layered amorphous structure. The MgSilHT sample calcined at 500 °C had a higher specific surface area (378 $m^2\ g^{-1}$) than MgSilSG. MgSilHT also possessed a larger specific pore volume than the MgSilSG. This is due to the MgSilHT sample having an ordered pentasil zeolite framework lattice with Mg and Si atoms. In addition, the substitution of some Mg(II) (0.65 Å) atoms in place of Si(IV) (0.41 Å) atoms in tetrahedron (TO_4) sites in the framework may result in unit cell expansion, resulting in higher specific surface areas and specific pore volumes. The samples nitridated at low temperatures, for instance MgSilSG30024 and MgSilHT30024, possess larger surface areas and pore volumes than the materials nitridated at higher temperatures, such as MgSilSG80024 and MgSilHT80048.

It was suggested by Wan et al. [27] that the loss of specific surface area is generally caused by the breaking of Si–O–Si bonds leading to partial collapse of the structure. Even so, XRD patterns did not show any specific change in the structure of the material or the presence of diffraction peaks due to any decomposed product of MgSil. Structural collapse could have taken place to some extent, resulting in the significant decrease of surface area and pore volume observed for the high-temperature nitridated samples. Partial collapse and loss of micropore structure was observed when the sample was heated at 800 °C for 24 h in air, the specific surface area reduced to 110 $m^2\ g^{-1}$ (Table 1). These observations indicate that the presence of NH_3 is likely to be an important factor in preserving the

Table 1 Specific surface area, pore volume, nitrogen content, and Hammett basic strength of calcined and nitridated magnesium slilicates samples

S. no.	Catalyst[a]	Specific surface area (m^2 g^{-1})	Specific pore volume (cm^3 g^{-1})	Nitrogen content[b] (wt%)	Hammett basic strength
1	MgSilSG500	320	0.45	–	$pK_b < 8.2$
2	MgSilSG800	110	0.14	–	$pK_b < 6.8$
3	MgSilSGN30024	310	0.30	1.3	$8.2\ pK_b < 10.1$
4	MgSilSGN50024	300	0.27	1.9	$11 < pK_b < 15$
5	MgSilSGN80024	200	0.17	2.7	$15 < pK_b < 17.4$
6	MgSilHT500	378	0.63	–	$pK_b < 8.2$
7	MgSilHT800	159	0.17	–	$pK_b < 6.8$
8	MgSilHTN30024	360	0.43	1.0	$8.2 < pK_b < 10.1$
9	MgSilHTN50024	352	0.38	1.3	$10.1 < pK < 15$
10	MgSilHTN80024	238	0.19	1.8	$11 < pK_b < 15$

[a] First three numbers in the catalyst code represents the nitridation temperature in °C and the last two numbers represents the treatment time in hours

[b] CHN analysis

main structure of MgSil during nitridation at high temperatures.

Figure 4 shows the pore-size distribution (PSD) plots obtained using the BJH equation from the desorption branch of the isotherm. The PSD measurements showed that all the samples had a PSD peak in the range of 10–11 nm pore diameter. Nitridation of MgSilSG and MgSilHT samples at 300 °C caused a broadening of the PSD peak. It is interesting to note that the development of mesopores was observed in the MgSilSG sample even though no template was used in the preparation of these materials. The mesopores observed in the SG samples could be due to interlayer spaces.

FTIR spectra of MgSilSG, MgSilHT samples calcined at 500 °C are shown in Fig. 5, spectra of SiO_2 and MgO are also included in this figure for the purpose of comparison. The SiO_2 sample exhibited bands at 3745 and 1620 cm^{-1} due to Si–OH groups and adsorbed water. The MgO sample exhibited a sharp band at 3700 cm^{-1}, which corresponds to the presence of Mg–OH groups. The spectra for the MgSilSG and MgSilHT samples showed all three aforementioned bands as well as a sharp band at 800 cm^{-1} and a broader band at 1080 cm^{-1}, which were attributed to asymmetric stretching vibrations of Si–O–Si and Si–O, respectively.

These results clearly show that the MgSilSG and MgSilHT samples exhibit characteristic vibrations for magnesium silicates. It is also possible to monitor the formation of different NH_x species on the surface of nitridated samples by FTIR spectroscopy [28]. The FTIR spectra of MgSilSG and MgSilHT samples nitridated for 24 h at 300, 500, and 800 °C are shown in Fig. 6a and b,

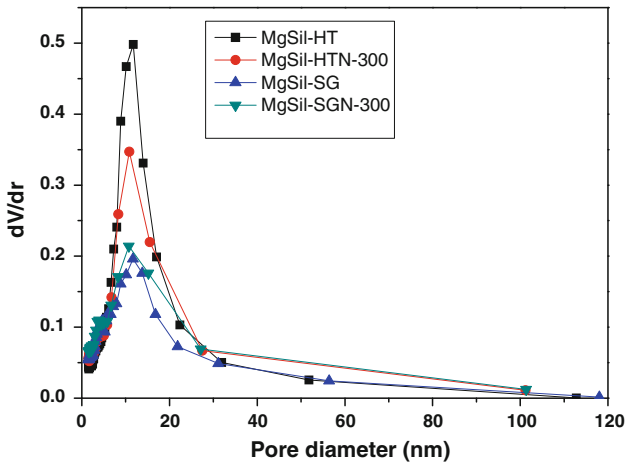

Fig. 4 Pore-size distribution patterns of selected magnesium silicate samples

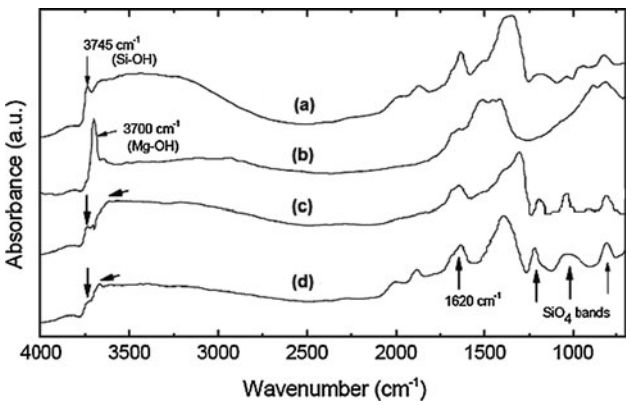

Fig. 5 FTIR spectra of (*a*) SiO_2, (*b*) MgO, (*c*) MgSilSG calcined at 500 °C, and (*d*) MgSilHT calcined at 500 °C

respectively. Two new bands at 1555 and 3410 cm^{-1} corresponding to symmetric bending vibration of the $–NH_2$ group and stretching mode of bridging NH moieties (–NH in Si–NH–Si) were observed in both the series of samples. The intensity of the bands at 3700 and 3745 cm^{-1} decrease with increasing nitridation temperature for all the samples analyzed. Also, the intensity of the band at 1620 cm^{-1} seems to decrease with increasing treatment temperature. The gradual disappearance of bands attributed to Si–OH and Mg–OH groups can be explained by the reaction between metal-OH and NH_3 to form metal $–NH_2$ groups during nitridation.

The thermal behavior of the nitridated samples was studied by simultaneous thermogravimetry–mass spectrometry (TG–MS). The MS analysis of the desorbed species revealed that H_2O ($m/e = 18$) and NH_3 ($m/e = 16$) are the major desorption species, with very minor amounts of O_2 and CO_2 which were likely adsorbed from the atmosphere during sample handling. At low temperatures, the mass loss is due to desorption of water. Ammonia desorption (due to hydrolysis) generally occurs in one or several stages, depending on the material nature. With the MgSilSG material nitridated at high temperature (800 °C), one broad weight loss is observed in the TG curve at around 150 °C which, according to the mass spectra, is due to desorption of both water and ammonia. The overlap between water and ammonia desorption peaks led us to perform a separate quantitative determination of ammonia from TG analysis. Again a relatively broad signal was observed around 150 °C with a shoulder on its high-temperature side (Fig. 7).

The relative peak area of this high-temperature shoulder increases with the increase of nitridation temperature. From the shape of the ammonia desorption curve one may be tempted to assume the existence of at least two different sites for NH_3 adsorption and that the density of the stronger sites increases with increasing nitridation temperature. Most interestingly, no further ammonia desorption is observed up to temperatures of 900 °C. From a semi-quantitative mass balance it can be concluded that the nitridated samples contain ca. 4–7 wt% nitrogen even after heating at 900 °C for several hours, probably in the form of terminal-NH_2 or bridging NH groups as evidenced by FTIR analysis.

A gradual increase in nitrogen content from 1.3 to 2.7 and 1.0 to 1.8 wt% in the cases of MgSilSG and MgSilHT, respectively, was observed upon increasing the nitridation temperature from 300 to 800 °C. It has been reported that nitridation of amorphous silicates at temperatures as low as 500 °C resulted in partial nitrogen incorporation, whereas at high temperatures more nitrogen is chemically bound to the surface as Si–NH–Si bridges, $Si–NH_2$ groups or just NH_3 molecules [29]. It is worth noting that the nitrogen incorporation capacity into both of the MgSilSG and the MgSilHT samples nitridated at different temperatures is higher than other microporous aluminosilicates, such as NaY and ZSM-5 [14]. This may be attributed to the layered structure of MgSilSG and ordered pentasil structure with higher crystal cell volume of MgSilHT samples. The

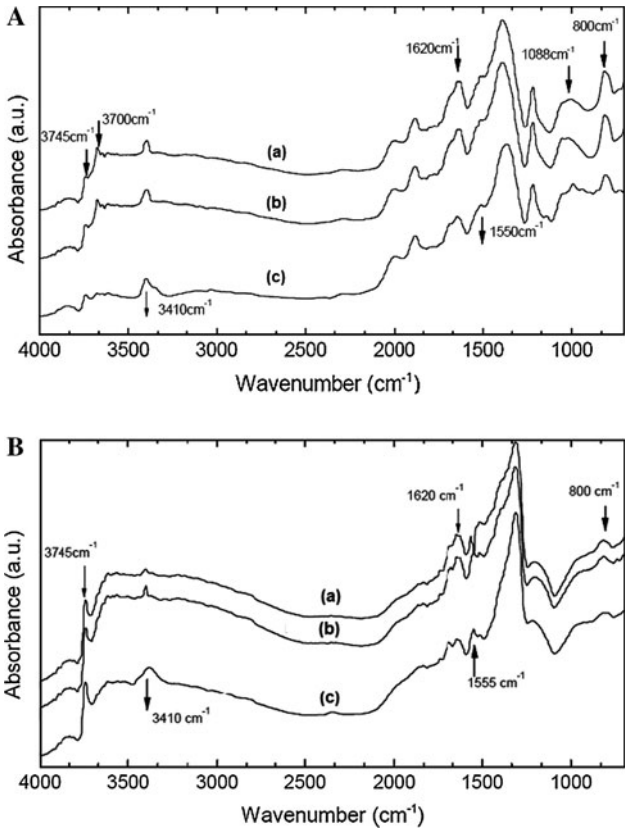

Fig. 6 **A** FTIR spectra for MgSilSG samples nitridated for 24 h at temperatures (*a*) 300 °C, (*b*) 500 °C, (*c*) 800 °C; **B** FTIR spectra for MgSilHT samples nitridated for 24 h at temperatures (*a*) 300 °C, (*b*) 500 °C, and (*c*) 800 °C

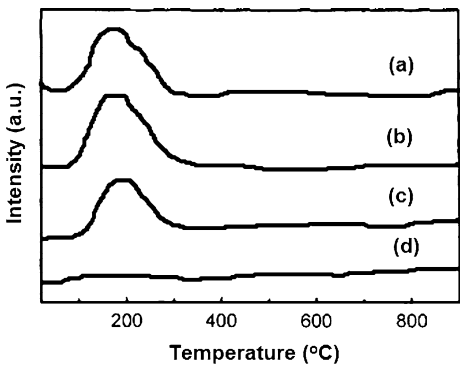

Fig. 7 Mass spectra obtained for $m/e = 16$ during temperature programmed heating of (*a*) MgSilHT80024, (*b*) MgSilSG80024, (*c*) MgSilSG50024, and (*d*) MgSilSG

nitrogen incorporation capacity for amorphous MgSilSG is greater than for the crystalline MgSilHT material. It is also reported that basicity of nitrogen-incorporated crystalline zeolites is weaker than that of the nitridized amorphous phase because it is quite difficult for zeolites to react with ammonia due to their crystallinity and instability of framework [13].

FTIR spectroscopy, TG–MS, and elemental analysis results reveal that at low temperatures, relatively small amounts of nitrogen was incorporated into the magnesium silicate framework, presumably via the formation Si–NH_2 or Mg–NH_2 species (Eqs. 1, 2) [30, 31]. At higher temperatures, a considerably higher amount of nitrogen was incorporated into the samples, most probably via the concomitant formation of Si–NH–Si or Si–NH_2–Mg species (Eqs. 3, 4) [32]. The decrease of intensity of the bands due to Si–O–Si and Si–O asymmetric stretching vibrations provides evidence for the incorporation of nitrogen into the MgSil framework. Wang et al. [23] reported that –NH– prefers to replace the oxygen atom in Si–O–Si rather than that in Si–OH, and consequently bridging –NH– species are the main basic species created by nitridation.

$$\mathrm{Si{-}OH + NH_3 \rightarrow Si{-}NH_2 + H_2O} \quad (1)$$

$$\mathrm{Mg{-}OH + NH_3 \rightarrow Mg{-}NH_2 + H_2O} \quad (2)$$

$$\mathrm{Si{-}NH_2 + H_2N{-}Si \rightarrow Si{-}N{-}SiH + NH_3} \quad (3)$$

$$\mathrm{Si{-}OH{-}Mg + NH_3 \rightarrow Si{-}NH_2{-}Mg + H_2O} \quad (4)$$

The surface of MgSil carries free hydroxyl groups (silanol groups), the most reactive groups on the surface. They provide the active sites for adsorption of organic and inorganic molecules and easily react chemically with multiple substituents. Being substituted with new atom groups, they provide potential for surface modification, which can be beneficial for catalysis [33]. MgSilSG and MgSilHT materials calcined at 500 °C possessed Hammett basicity of $pK_b < 8.2$. Calcination at 800 °C changed the structural properties of both materials, as evidenced by decreased surface area and base strength (Table 1). The change is likely associated with the loss of surface hydroxyl groups and fragmentation of the framework, which could fracture the crystallites. Nitridation with ammonia increased the basic strength of both MgSil materials. A gradual increase of basic strength was observed with increase of nitridation temperature from 300 to 800 °C. These results are in accordance with the elemental analysis.

We have not found any research dealing with synthesis, characterization, and evaluation of nitridated MgSil materials as basic catalysts. Therefore, we used the Knoevenagel condensation, which is a simple, frequently employed test reaction for basic catalysts, for the catalytic evaluation of the novel materials prepared in the course of this study. Benzylidene malononitrile was observed as the sole reaction product, aside from water. The conversion of benzaldehyde is dependent upon reaction time (see Table 2; Fig. 8). The parent oxides SiO_2 and MgO of magnesium silicates are less active than both the MgSilSG and the MgSilHT samples. SiO_2 and MgO gave 26 and 39 % conversion of benzaldehyde after 7 h of reaction. MgSilSG showed an excellent performance, resulting in a 78.2 % conversion, whilst MgSilHT only offered 60.3 % after 7 h of reaction time.

It was found that the MgSilSG and MgSilHT samples nitridated at 300 and 500 °C were more active for the Knoevenagel condensation than the pure magnesium silicates. The activity of the catalysts decreased with increasing nitridation temperature from 300 to 800 °C (Fig. 8). The sample MgSilSGN30024 shows a conversion of 83 % after 1 h, whereas the conversion was only 72 % for the MgSilSGN80024 sample. After 4 h, the conversion was increased to 94 and 82 % when the samples MgSilSGN30024 and MgSilSGN80024 were used, respectively. A similar behavior was observed in the case of nitridated MgSilHT samples. Layer structured nitridated MgSilSG samples offered higher conversions than nitridated pentasil type crystalline MgSilHT samples.

It is clear from the nitrogen physisorption data (Table 1) that the BET surface area and pore volume of most active catalyst (MgSilSGN30024) was 310 $m^2\ g^{-1}$ and 0.30 $cm^3\ g^{-1}$, respectively. However, its counterpart MgSilHTN30024 shows less activity but possesses a high BET surface area 360 $m^2\ g^{-1}$ with pore volume of 0.43 $cm^3\ g^{-1}$. This indicates that the large surface area and porosity are not indispensable in this reaction system.

In general, the reaction should take place near the pore-mouth of the silicates, not deep inside the pore. The efficient catalysis by layered materials may be due to the more

Table 2 Conversion of benzaldehyde (X_{BA}) on parent precursors and calcined magnesium silicates

X_{BA} (%)[a]	Catalyst			
	SiO_2	MgO	MgSilSG	MgSilHT
Reaction time, 1 h	10.0	14.5	47.5	20.8
Reaction time, 2 h	20.5	21.8	52.4	27.8
Reaction time, 3 h	24.5	23.9	62.6	34.9
Reaction time, 4 h	25.0	28.0	67.8	43.1
Reaction time, 5 h	25.7	35.0	71.9	48.4
Reaction time, 6 h	25.8	39.0	75.6	52.6
Reaction time, 7 h	26.0	39.0	78.2	60.3

[a] Conversion of benzaldehyde; reaction conditions: benzaldehyde (4 mmol), malononitrile (4 mmol), and 10 mL of toluene, 200 mg of catalyst; reaction temperature: 80 °C

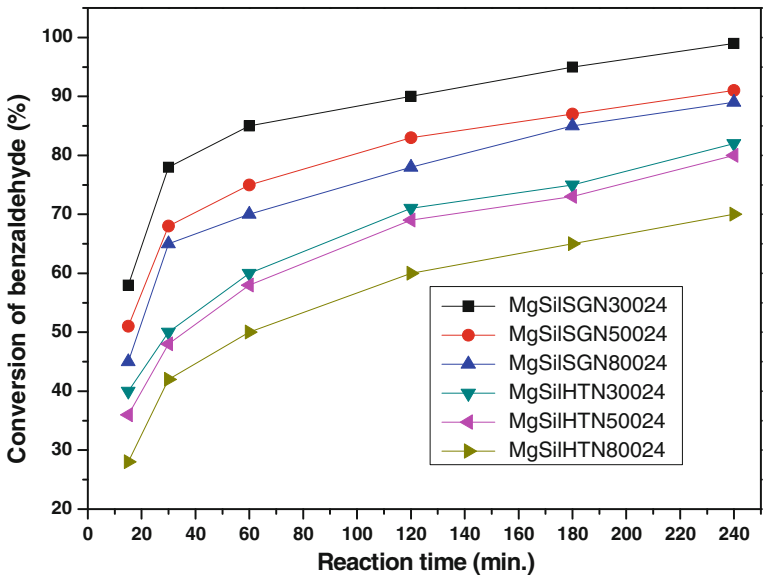

Fig. 8 Conversion of benzaldehyde over MgSilSG and MgSilHT samples nitridated for 24 h at different temperatures

exposed catalytic sites at the pore-mouth as compared to crystalline materials. This means that the good accessibility to the acidic and basic species-silicate interface is necessary for the activation of substrates. Considering that the MgSilSG structures contained more nitrogen incorporation after nitridation than the MgSilHT materials, it was reasonable to conclude that the distinct differences in catalytic activity were caused by the differences in their structures.

The apparent broadening of the XRD peaks in the case of MgSilSG samples indicates the small crystal sizes of the obtained materials. Smaller crystals/particles offer shorter intracrystalline diffusion paths for the reactants and products, and possess a higher number of external active sites compared to larger crystals [34].

Ernst et al. [17] observed nitridated ZSM-5 catalysts are less active than other crystalline aluminosilicates, NaY, NaX, and aluminophosphates. Activity results of the Knoevenagel condensation for MgSil, nitridated MgSil, and different zeolite structures are summarized in Table 3. It is noteworthy that nitridated MgSil catalysts showed higher catalytic activity than nitridated NaX, NaY, ZSM-5, and $AlPO_4$ under similar reaction conditions.

Nitridated MgSil catalysts offered lower catalytic activity than zeolite beta; this could be due to the structural differences between zeolite beta and MgSil materials. Zeolite beta possesses a unique, defective crystalline structure, which is responsible for high nitrogen incorporation at low temperatures [24]. The selectivity for benzylidine malononitrile is close to 100 % for all the samples, with no other reaction product due to excessive condensation (which involves the reaction of benzylidine malononitrile with another malononitrile molecule). Although the catalysts prepared at high nitridation temperatures showed more nitrogen incorporation, they are less active than the nitridated catalysts prepared at low temperatures. This implies that the rate of the Knoevengel condensation is not just dependent upon the nitrogen content or the basic nature of the catalyst.

Table 3 Conversion of benzaldehyde (X_{BA}) over nitridated catalysts with different structures

S. no.	Catalyst[a]	X_{BA} (%)[b]	References
1	MgSilSGN 30024	83	This study
2	MgSilSGN 50024	70	This study
3	MgSilHTN 30024	60	This study
4	MgSilHTN 50024	60	This study
5	MgSilSGM 80024	70	This study
6	MgSilHTN 80024	50	This study
7	Beta zeolite 30024	98	[24][c]
8	Beta zeolite 50024	84	[24]
9	NaY 80024	15	[17][c]
10	NaX 85024	52	[17]
11	ZSM-5 85036	6	[17]
12	$AlPO_4$ 87536	50	[17]

[a] First three numbers in the catalyst code represents the nitridation temperature in °C and the last two numbers represents the treatment time in hours

[b] Conversion of benzaldehyde; reaction conditions: benzaldehyde (4 mmol), malononitrile (4 mmol), and 10 mL of toluene, 200 mg of catalyst; reaction temperature: 80 °C; reaction time: 60 min

[c] The reaction conditions are same as in this study

Weitkamp et al. [35] described how organic amines are attached to a mesoporous silica surface and also illustrated how the Knovenagel condensation reaction between benzaldehyde and active methylene compounds takes place on such a modified surface (Scheme 1). The reaction is

Scheme 1 Plausible Knoevenagel condensation reaction mechanism on nitridated magnesium silicate catalysts

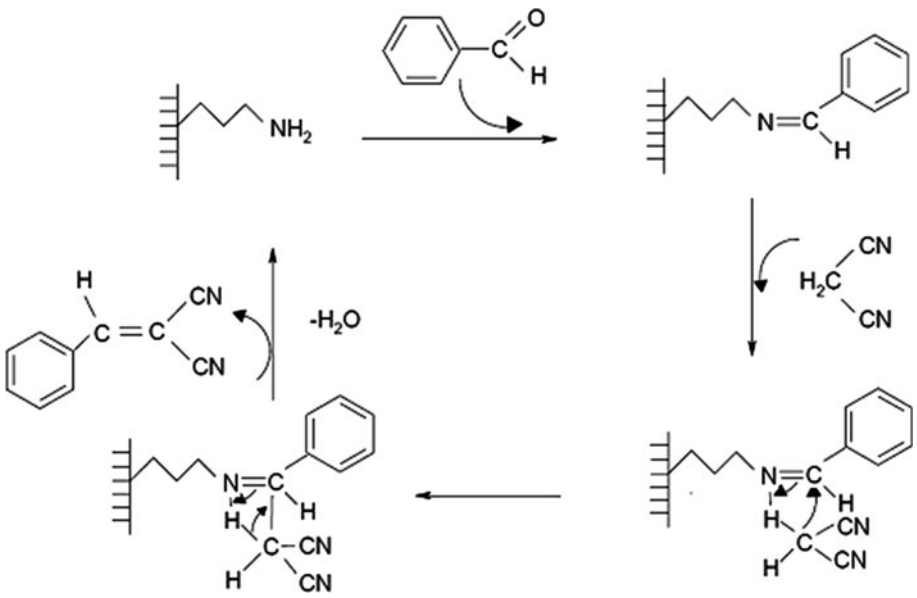

initiated on Bronsted-basic sites (organic amine), when a benzaldehyde molecule reacts with the surface amine to form an imine compound.

The addition of the active methylene group and the subsequent molecular rearrangement produces the condensation product and one molecule of water. It has also been reported [36] that aluminophosphate catalysts containing acid and basic sites are active in the Knoevenagel condensation of heptanal with benzaldehyde, exhibiting higher rates and selectivities, compared to solid acid or basic catalysts alone. The authors proposed a mechanism involving the interaction of an acid site with the carbonyl group of benzaldehyde, which leads to a polarization of the carbon–oxygen bond and thereby increases the positive charge on the carbon supporting the carbonyl group. Hence, this carbon becomes more susceptible to the attack by the carbanion, which is formed by the interaction of the methylene compound with the basic oxygen sites.

Ernst et al. [17] also observed that the presence of hydroxyl groups seems to be inevitable for the catalytic activity of the nitridated aluminosilicate materials for Knoevenagel condensations, because the nitridated catalyst did not show any activity in the absence of moisture. In accordance with these observations, the influence of silanol groups on the catalytic activity of nitridated zeolites, a tentative reaction mechanism was adapted from the literature [36]. A reason for the higher catalytic activity observed with the MgSilSG samples was that they possessed more silanol groups than the MgSilHT samples (from FTIR spectra). It was important to ensure that dissolved ammonia (which could eventually form via hydrolysis of Si–NH_2 or Mg–NH_2 groups in the presence of water during the reaction) did not contribute to the observed catalytic activity; therefore, the MgSilSG30024 catalyst was removed by filtration from the hot reaction mixture, washed with toluene, and subsequently dried at 150 °C. It was then added to a fresh reaction solution to carry out the routine reaction. The catalytic activity observed was comparable to that in the initial experiment. This observation indicates that –NH_2 groups are not hydrolyzing to ammonia.

Conclusions

Amorphous and crystalline MgSil materials were prepared by sol–gel and hydrothermal methods. They were nitridated via ammonia treatment at temperatures from 300 to 800 °C for 24 h. From TG–MS, elemental analysis, and FTIR spectroscopic characterization of the nitridated samples, it can be concluded that the incorporated amount of nitrogen increases with increasing nitridation temperature. Moreover, the FTIR spectra suggest the formation of basic nitride species for both series of MgSil samples, which were ammonia-treated at a temperature of 800 °C. In contrast, both basic –NH_2 species and acidic Si–OH species have been identified in the catalysts that were nitridated at temperatures 300 and 500 °C. Magnesium silicates, when nitridated at 300 °C for 24–48 h exhibit a surprisingly high catalytic activity for the Knoevenagel condensation of benzaldehyde with malononitrile. Higher nitridation temperatures lead to lower activities. This suggests that the catalytic activity of nitridated MgSil materials does not depend only on the nitrogen content of the samples; the nature of the framework nitrogen species plays an important role. From our results presented here, it can be concluded that both acidic (namely Si–OH, Mg–OH) and basic (namely Si–NH_2) sites are required to obtain

high catalytic activity for Knoevenagel condensation reaction.

Acknowledgements This work was funded by the Deanship of Scientific Research (DSR), King Abdulaziz University, Jeddah, under Grant No. (130-021-D1433). The authors, therefore, acknowledge with thanks DSR technical and financial support. Authors also thank Desert Baker for her technical support.

References

1. Corma A (1997) Chem Rev 97:2373. doi:10.1021/cr960406n
2. Eduardo Ruiz-Hitzky J (2001) Mater Chem 11:86. doi:10.1039/b003197f
3. Murray HH (1999) Clay Miner 34:39. doi:10.1180/000985599546055
4. Le Van MaoR, Rutinduka E, Detellier C, Gougay P, Hascoet V, Tavakoliyan S, Hoa SV, Matsuura T (1999) J Mater Chem 9:783. doi:10.1039/a806624h
5. Damyanova S, Daza L, Fierro JLG (1996) J Catal 159:150. doi:10.1006/jcat.1996.0074
6. Zhu J, Morgan AB, Lamelas FJ, Wilkie CA (2001) Chem Mater 13:3774. doi:10.1021/cm000984r
7. Sandi G, Winans RE, Seifert S, Carrado KA (2002) Chem Mater 14:739. doi:10.1021/cm010627w
8. Wenxing K, Facey GA, Detellier C, Casal B, Serratosa JM, Ruiz-Hitzky E (2003) Chem Mater 15:4956. doi:10.1021/cm034867i
9. Graces JM (1988) US Patent No. 4,732,747
10. Corma A, Martin-Aranda RM (1991) J Catal 130:130. doi:10.1016/0021-9517(91)90097n
11. Barthomeuf D (1996) Catal Rev Sci Eng 38:521. doi:10.1080/01614949608006465
12. Chorley RW, Lednor PW (1991) Adv Mater 3:474. doi:10.1002/adma.19910031004
13. Lednor PW, de Ruiter R (1991) J Chem Soc Chem Commun. 1625. doi:10.1039/C39910001625
14. Lednor PW (1992) Catal Today 15:2243. doi:10.1016/0920-5861(92)80178p
15. Kerr GT, Shipman GF (1968) J Phys Chem 72:3071. doi:10.1021/j100854a084
16. Yamamoto K, Sakata Y, Nohara Y, Takahashi Y, Tatsumi T (2003) Science 300:470. doi:10.1126/science.1081019
17. Ernst S, Hartmann M, Sauerbeck S, Bongers T (2000) Appl Catal A Gen 200:117. doi:10.1016/S0926-860X(00)00646-3
18. Han AJ, Guo J, Yu H, Zeng Y, Huang YF, He HY, Long YC (2006) ChemPhysChem 7:607. doi:10.1002/cphc.200500389
19. El Haskouri J, Cabrera S, Sapina F, Latorre J, Guillem C, Porter AB, Porter DB, Marcos MD, Amoros P (2001) Adv Mater 13:192. doi:10.1002/1521-4095(200102
20. Wu G, Jiang S, Li L, Guan N (2010) Appl Catal A Gen 391:225. doi:10.1016/j.apcata.2010.07.033
21. Chino N, Okubo T (2005) Microporous Mesoporous Mater 87:15. doi:10.1016/j.micromeso.2005.07.034
22. Hammond KD, Dogan F, Tompsett GA, Agarwal V, Conner WC Jr, Grey CP, Auerbach SM (2008) J Am Chem Soc 12:14912. doi:10.1021/ja8044844
23. Wang T, Wu G, Guan N, Li L (2012) Microporous Mesoporous Mater 148:184. doi:10.1016/j.micromeso.2011.07.024
24. Narasimharao K, Hartmann M, Thiel HH, Ernst S (2005) Microporous Mesoporous Mater 90:377. doi:10.1016/j.micromeso.2005.11.029
25. Tracey MMJ, Higgins JB (2001) Collection of simulated XRD powder patterns for zeolites, 4th edn. Structure Commission of the International Zeolite Association. Elsevier, Amsterdam, p. 367
26. Kitayama Y, Satoh M, Kodama T (1996) Catal Lett 36:95. doi:10.1007/BF00807211
27. Wan K, Liu Q, Zhang C (2003) Chem Lett 32:362. doi:10.1246/cl.2003.362
28. Frost RL, Ding Z (2003) Thermochim Acta 397:119. doi:10.1016/S0040-6031(02)00228-9
29. Ying JY, Mehnert CP, Wong MS (1999) Angew Chem Int Ed 38:56. doi:10.1002/(SICI)1521-3773(1999)115
30. Grange P, Bastians P, Conanec R, Marchand R, Laurent Y (1994) Appl Catal A Gen 114:L191. doi:10.1016/0926-860X(94)80172-X
31. Fink P, Datka J (1989) J Chem Soc Faraday Trans 1(85):3079. doi:10.1039/F19898503079
32. Angeletti E, Canepa C, Martinetti G, Venturello P (1989) J Chem Soc Perkin Trans 1:105. doi:10.1039/P19890000105
33. Wang M, Deb S, Bonfield W (2000) Mater Lett 44:119. doi:10.1016/S0167-577X(00)00026-4
34. Kim JH, Kunieda T, Niwa M (1998) J Catal 173:433. doi:10.1006/j.cat.1997.1950
35. Weitkamp J, Hunger M, Rymsa U (2001) Microporous Mesoporous Mater 48:255. doi:10.1016/S1387-1811(01)00366-3
36. Climent MJ, Corma A, Fornes V, Guil-Lopez R, Iborra S (2002) Adv Synth Catal 344:1090. doi:10.1002/1615-4169(200212)344